The official journal of the Japan Atherosclerosis Society and
the Asian Pacific Society of Atherosclerosis and Vascular Diseases

Original Article

J Atheroscler Thromb, 2019; 26: 246-259. http://doi.org/10.5551/jat.44040

Loss of ACAT1 Attenuates Atherosclerosis Aggravated by Loss of NCEH1 in Bone Marrow-Derived Cells

Hisataka Yamazaki[1], Manabu Takahashi[1], Tetsuji Wakabayashi[1], Kent Sakai[1], Daisuke Yamamuro[1], Akihito Takei[1], Shoko Takei[1], Shuichi Nagashima[1], Hiroaki Yagyu[1], Motohiro Sekiya[2], Ken Ebihara[1] and Shun Ishibashi[1]

[1]Division of Endocrinology and Metabolism, Department of Medicine, Jichi Medical University, Tochigi, Japan
[2]The Department of Diabetes and Metabolic Diseases, Graduate School of Medicine, The University of Tokyo, Tokyo, Japan

Aim: Acyl-CoA cholesterol acyltransferase 1 (ACAT1) esterifies free cholesterol to cholesteryl esters (CE), which are subsequently hydrolyzed by neutral cholesterol ester hydrolase 1 (NCEH1). The elimination of ACAT1 *in vitro* reduces the amounts of CE accumulated in *Nceh1*-deficient macrophages. The present study aimed at examining whether the loss of ACAT1 attenuates atherosclerosis which is aggravated by the loss of NCEH1 *in vivo*.

Methods: *Low density lipoprotein receptor* (*Ldlr*)-deficient mice were transplanted with bone marrow from wild-type mice and mice lacking ACAT1, NCEH1, or both. The four types of mice were fed a high-cholesterol diet and, then, were examined for atherosclerosis.

Results: The cross-sectional lesion size of the recipients of *Nceh1*-deficient bone marrow was 1.6-fold larger than that of the wild-type bone marrow. The lesions of the recipients of *Nceh1*-deficient bone marrow were enriched with MOMA2-positive macrophages compared with the lesions of the recipients of the wild-type bone marrow. The size and the macrophage content of the lesions of the recipients of bone marrow lacking both ACAT1 and NCEH1 were significantly smaller than the recipients of the *Nceh1*-deficient bone marrow, indicating that the loss of ACAT1 decreases the excess CE in the *Nceh1*-deficient lesions. The collagen-rich and/or mucin-rich areas and *en face* lesion size were enlarged in the recipients of the *Acat1*$^{-/-}$ bone marrow compared with those of the recipients of the WT bone marrow.

Conclusion: The loss of ACAT1 in bone marrow-derived cells attenuates atherosclerosis, which is aggravated by the loss of NCEH1, corroborating the *in vitro* functions of ACAT1 (formation of CE) and NCEH1 (hydrolysis of CE).

Key words: Cholesterol, Atherosclerosis, Macrophage, Inflammation, Foam cells

Introduction

Monocytes/macrophages are critically involved in several phases of atherosclerosis: initiation, progression, plaque rupture, regression, and resolution[1)]. In the early stage of atherosclerosis, monocytes infiltrate into subendothelial spaces of arterial walls, take up modified lipoproteins, and transform into cholesteryl esters (CE)-laden macrophages, referred to as foam cells.

After the endocytosis of lipoproteins, the CE in the lipoproteins are initially hydrolyzed to free cholesterol (FC) and fatty acid in the lysosome. The excess of FC is re-esterified by acyl-CoA: cholesterol acyltransferase(ACAT), also known as sterol O-acyltransferase (SOAT), to form CE in the endoplasmic reticulum for storage in the cytoplasmic lipid droplets[2)]. Two ACAT

Address for correspondence: Shun Ishibashi, Division of Endocrinology and Metabolism, Department of Internal Medicine, Jichi Medical University, 3311-1 Yakushiji, Shimotsuke, Tochigi 329-0498, Japan E-mail: ishibash@jichi.ac.jp

Received: December 25, 2017 Accepted for publication: June 28, 2018

isoforms have been identified in mammals: ACAT1 and ACAT2. ACAT1 is ubiquitously expressed, especially in steroidogenic organs and macrophages, while ACAT2 is expressed exclusively in intestinal epithelial cells and hepatocytes where it is involved in lipoprotein assembly and secretion.

The hydrolysis of intracellular CE is the initial step of reverse cholesterol transport[3]. The enzymes hydrolyzing CE at neutral pH have been collectively called neutral CE hydrolases (NCEHs)[4]. Under certain circumstances, lysosomal acid lipase may be involved in reverse cholesterol transport, because of the potential involvement of autophagy[5]. We have shown previously that neutral cholesterol ester hydrolase 1 (NCEH1)[6, 7], also known as KIAA1363 or arylacetamide deacetylase-like 1, is responsible for most of the activity in human monocyte-derived macrophages[8] and half of the activity in mouse peritoneal macrophages, where the rest of the activity is mediated by hormone-sensitive lipase (HSL, LIPE)[9-11]. The overexpression of NCEH1 inhibited the accumulation of CE in THP-1 macrophages[6]. Conversely, the pharmacological and genetic inhibition of NCEH1 increased the accumulation of CE in peritoneal macrophages treated with acetylated low density lipoproteins (acLDL)[9, 10]. In an experiment in which mice deficient in *LDL receptor* ($Ldlr^{-/-}$) were transplanted with bone marrow from wild-type (WT) and $Nceh1^{-/-}$ mice and, then, fed a with high-cholesterol diet[9], the recipients of the $Nceh1^{-/-}$ bone marrow developed larger atherosclerotic lesions than the recipients of the WT bone marrow[9].

Aim

To test whether the elimination of ACAT1 in the macrophages mitigates the worsening of atherosclerosis in $Ldlr^{-/-}$ mice whose bone marrow is transplanted from $Nceh1^{-/-}$ mice, we transplanted bone marrow from WT and mice which lack NCEH1, ACAT1 or both to $Ldlr^{-/-}$ mice and we compared the degree of atherosclerosis after feeding them a high-cholesterol diet.

Methods

Animals

$Acat1^{-/-}$ [12] and $Nceh1^{-/-}$ mice[9] were generated as described previously. Mice lacking both ACAT1 and NCEH1 ($Acat1^{-/-};Nceh1^{-/-}$) were generated by mating these mice. The littermate WT were used as a control. All the mice used in this study, including the $Ldlr^{-/-}$ mice[13] were crossed onto C57BL/6 mice more than ten times. Genotyping was performed via PCR using genomic DNA isolated from the tail tip. The mice were maintained with 12 h light/dark cycle. Two diets were used: i) a normal chow diet containing 4.4% (w/w) fat and 25.3% (w/w) protein (CE-2, Japan CLEA); ii) a high-cholesterol diet (HCD) containing 1.25% (w/w) cholesterol and 15% (w/w) cocoa butter and 0.5% (w/w) cholic acid (Oriental Yeast Company). Animal care and experimental procedure were performed according to the regulations of Jichi Medical University.

Bone Marrow Transplantation

Eight-week-old female recipient $Ldlr^{-/-}$ mice were irradiated 9 Gy to eliminate endogenous bone marrow-derived cells. The bone marrow cells was collected by flushing the femurs and tibias of 8-week-old male WT, $Acat1^{-/-}$, $Nceh1^{-/-}$, $Acat1^{-/-};Nceh1^{-/-}$ donor mice. The irradiated recipient mice were transplanted with 5×10^6 bone marrow cells by tail vein injection 24 h later. Thereafter, the mice were fed on a chow diet for first 4 weeks, then, were fed HCD for 12 weeks. The recipient mice had free access to water that was acidified to pH 2.6 for the prevention of infection. In addition, 1 week before and 2 weeks after radiation, 100 mg/L neomycin (Sigma) and 10 mg/L polymyxin B sulfate (Sigma) were added to the water. After feeding with HCD, the transplanted mice were euthanized for the assessment of the atherosclerotic lesions.

The hematopoietic reconstitution of recipient mice was determined in genomic DNA from bone marrow by PCR. The sex of the bone marrow of donor mice was determined in Sry gene primers. The primers for *Acat1*, *Nceh1* were used to detect both the WT and mutant genes.

Plasma Lipids and Lipoproteins

After a 16-h fast, blood was collected into tubes containing EDTA for the separation of plasma. Kits (Determiner TC Ⅱ, Kyowa Medex and L-Type TG M, Wako) were used to determine the plasma levels of total cholesterol (TC) and triglyceride (TG) enzymatically. High performance liquid chromatography (HPLC) analyses of plasma were performed, as described previously[14].

Quantification of Atherosclerotic Lesions

After feeding with HCD, the mice were euthanized and their aorta and hearts were isolated for the evaluation of cross-sectional lesion area at the aortic roots and *en face* atherosclerotic lesion area of the aorta. The cross-sectional lesion area was evaluated according to the method of Paigen *et al.*[15] with slight modifications. In brief, the heart was perfused with saline containing 4% (w/v) formalin, and was fixed for more than 48 h in the same solution. The basal half of the heart was embedded in Tissue-Tek OCT compound (Sakura Finetek), and serial sections were cut using

Table 1. Body weight and plasma levels of lipids

Time (weeks)	Genotype BM	n	Weight (g)	Total cholesterol (mg/dl)	Triglyceride (mg/dl)
	Acat1 Nceh1				
0	+/+ +/+	14	16.7 ± 1.4	322 ± 51	200 ± 120
	−/− +/+	13	17.0 ± 1.3	337 ± 68	183 ± 64
	+/+ −/−	18	16.6 ± 1.0	336 ± 53	235 ± 106
	−/− −/−	15	17.2 ± 0.8	321 ± 47	245 ± 93
12	+/+ +/+	14	19.3 ± 1.9	1049 ± 173	152 ± 51
	−/− +/+	13	20.3 ± 1.2	1078 ± 213	123 ± 72
	+/+ −/−	18	19.3 ± 1.6	1136 ± 207	134 ± 62
	−/− −/−	15	19.7 ± 1.7	1135 ± 195	168 ± 58

cryostat (6 μm thick), as described previously[12, 15]. Four sections, each separated by 60 μm, were used to evaluate the lesions; two at the end of the aortic sinus and two at the junctional site of sinus and ascending. The sections were stained with Oil red O (ORO) and counterstained with hematoxylin to quantify the atherosclerotic plaque area and the neutral lipid positive area. The *en face* lesion area of the aorta was evaluated as described previously[9]. In brief, the aorta was opened from the aortic root to the iliac bifurcation, and was pinned out flat on a wax surface. Atheromatous plaques in the aorta were visualized by staining with Sudan Ⅳ, and the luminal side of the stained aorta was photographed. Adobe Photoshop 6 image analysis software was used to perform the image capture and analysis. The extent of atherosclerosis was expressed as the percent of surface area of the entire aorta covered by lesions.

Histology

The sections were stained with hematoxylin and eosin (HE), Movat's pentachrome[16], or Masson trichrome[17]. HE staining was used to determine the size of the necrotic core. Immunostaining was performed as described previously[9, 18]. In brief, the sections were incubated with the primary antibody against mouse MOMA-2 (1:600; Bio-Rad) or α-SMA (1:100; abcam) overnight at 4℃. After washing, the sections were incubated with biotinylated anti-rat antibody (1:200; Vector Labs) or anti-rabbit antibody (1:200; Vector Labs) for 2 h at 37℃, and then with avidin-biotin peroxidase complex (Vector Labs) for 30 min. Last, the sections were developed with 3, 3'-diaminobenzidine tetrahydrochloride (DAB) (Sigma), and counterstained with hematoxylin.

Preparation of Peritoneal Macrophages

Peritoneal macrophages were obtained 3 days after the intraperitoneal injection of 2 ml of 5% thioglycollate broth. The macrophages (2×10^6) were plated to each well of 12-well plates, and were cultured in Dulbecco's modified Eagle's medium (DMEM) supplemented with 10% (v/v) fetal bovine serum and antibiotics for 3 h. Thereafter, the non-adherent cells were washed with PBS.

Preparation of Lipoproteins

Blood was drawn from healthy volunteers and LDL (d = 1.019−1.063 g/ml) and lipoprotein deficient serum (LPDS; d > 1.21) were isolated by ultracentrifugation[19]. LDL was acetylated with acetic anhydrate as described previously[20]. Protein concentrations were determined by the BCA kit (Pierce).

CE Formation Assay

Following a 24-h incubation period in medium containing 5 mg/ml of LPDS, mouse peritoneal macrophages were incubated with 100 μg/ml of acLDL, 5 mg/ml of BSA, and 0.1 mM [1-^{14}C]oleate-albumin complex at 37℃ for 24 h. CE formation was determined as described previously[21].

Cellular Neutral Lipids

The macrophages were incubated with 100 μg/ml of acLDL in DMEM containing 5 mg/ml of BSA for 24 h in a Lab-Tek Ⅱ Chamber slide system (Thermo Scientific). After having been fixed with 4% paraformaldehyde, the macrophages were stained with Oil red O.

Statistics

The data were presented as means ± S.D. The one way analysis of variance (ANOVA) was used for multiple comparisons. When the ANOVA results were statistically significant (i.e., $p < 0.05$), then, individual comparisons were made with the Tukey post-hoc test.

Results

To assess the role of ACAT1 in the worsening of atherosclerosis in the *Ldlr*$^{-/-}$ mice whose bone marrow was transplanted with that from *Nceh1*$^{-/-}$ mice, we transplanted the bone marrow obtained from male WT, *Acat1*$^{-/-}$, *Nceh1*$^{-/-}$, *Acat1*$^{-/-}$;*Nceh1*$^{-/-}$ mice into female *Ldlr*$^{-/-}$ mice which were irradiated to eliminate the endogenous bone marrow. Four weeks after the transplantation, the recipient mice were fed HCD for 12 additional weeks.

PCR-assisted amplification of the *Sry* gene (a male marker) and *Acat1* or *Nceh1* mutant gene was used to verify the successful reconstitution of recipients with cells of donor origin after the bone marrow transplantation (**Supplemental Fig. 1**).

Bone marrow specific inactivation of the *Acat1* and/or *Nceh1* gene did not significantly affect the body weight, plasma lipids and lipoprotein fractions in *Ldlr*$^{-/-}$ mice before and after feeding with HCD (**Table 1** and **Supplemental Fig. 2**). All the types of mice developed severe hypercholesterolemia.

After feeding with HCD for 12 weeks, atherosclerosis was evaluated by cross-sectional analysis of aortic roots and the *en face* surface lesion area of the aorta. Regarding the size of the cross-sectional lesions (**Fig. 1**), there was no difference between the recipients of the WT bone marrow and those of the *Acat1*$^{-/-}$ bone marrow. The recipients of *Nceh1*$^{-/-}$ bone marrow showed a 1.6-fold increase in the lesions compared with those of the WT bone marrow. The recipients of the *Acat1*$^{-/-}$;*Nceh1*$^{-/-}$ bone marrow showed a significant decrease of the lesions to a level indistinguishable from the recipients of the WT and *Acat1*$^{-/-}$ bone marrow.

Regarding the size of *en face* lesion area (**Supplemental Fig. 3**), the recipients of the *Acat1*$^{-/-}$ bone marrow showed a 2.2-fold increase compared with those of the WT bone marrow. The recipients of the *Nceh1*$^{-/-}$ bone marrow showed a 2.1-fold increase in the lesions compared with those from the WT bone marrow ($p<0.01$). There was no difference between the recipients of the *Acat1*$^{-/-}$ and *Nceh1*$^{-/-}$ bone marrows. The lesion size of the recipients of the *Acat1*$^{-/-}$;*Nceh1*$^{-/-}$ bone marrow was not significantly different from either that of the *Acat1*$^{-/-}$ bone marrow or the *Nceh1*$^{-/-}$ bone marrow.

To determine the characteristics of the lesions, we employed several different ways to stain the cross-sectional sections (**Figs. 2** and **3**). ORO staining was performed to visualize neutral lipids, mostly CE, accumulated in the lesions. The percentage of the ORO-positive area of the recipients of the *Acat1*$^{-/-}$ bone marrow was significantly smaller than that of the WT bone marrow by 44% ($p<0.01$) (**Fig. 3A**). The percentage of the ORO-positive area of the recipients of *Nceh1*$^{-/-}$ bone marrow was larger than that of the WT bone marrow by 34% ($p<0.05$). The percentage of the ORO-posi-

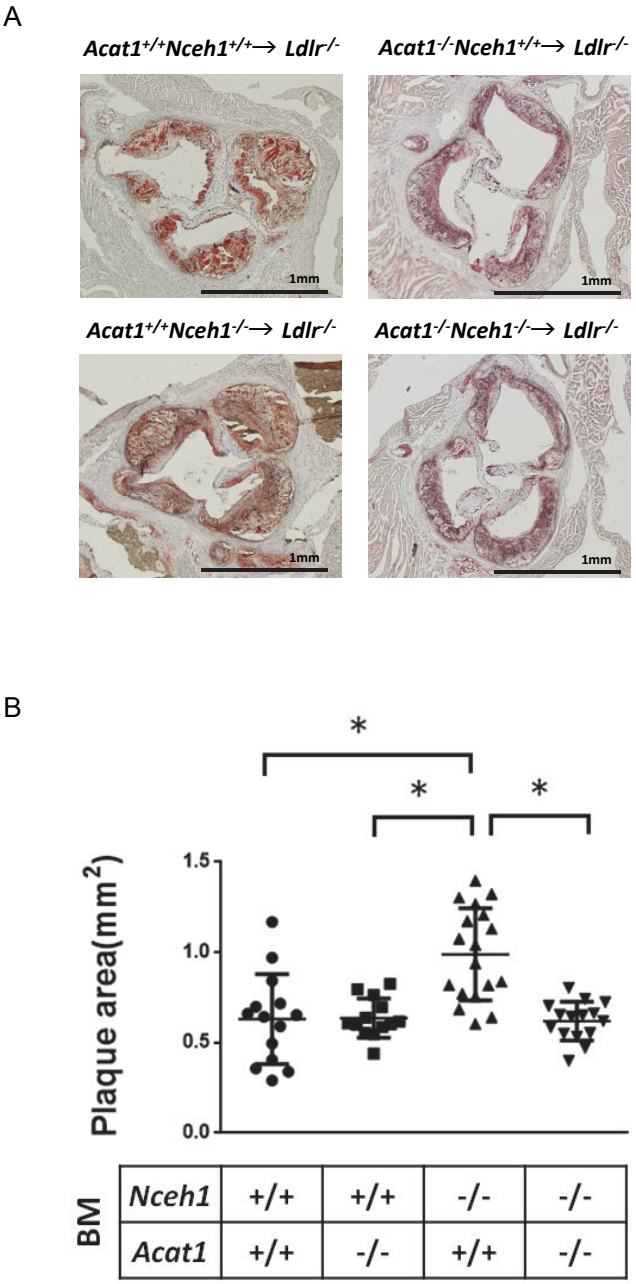

Fig. 1. Cross-sectional atherosclerotic lesions in *Ldlr*$^{-/-}$ mice transplanted with *Acat1*$^{-/-}$, *Nech1*$^{-/-}$, *Acat1*$^{-/-}$;*Nech1*$^{-/-}$ bone marrow.

Irradiated female 8-week-old *Ldlr*$^{-/-}$ mice ($n=13-18$) were transplanted with WT, *Acat1*$^{-/-}$, *Nceh1*$^{-/-}$, *Acat1*$^{-/-}$;*Nech1*$^{-/-}$ bone marrow. Four weeks after feeding on a chow diet, mice were fed on a high-cholesterol diet (HCD) for 12 weeks. (A) Representative images of Oil red O staining of the cross-sections in the aortic sinus. (B) Quantified lesion areas. Values are expressed as means ± SD. *$p<0.001$.

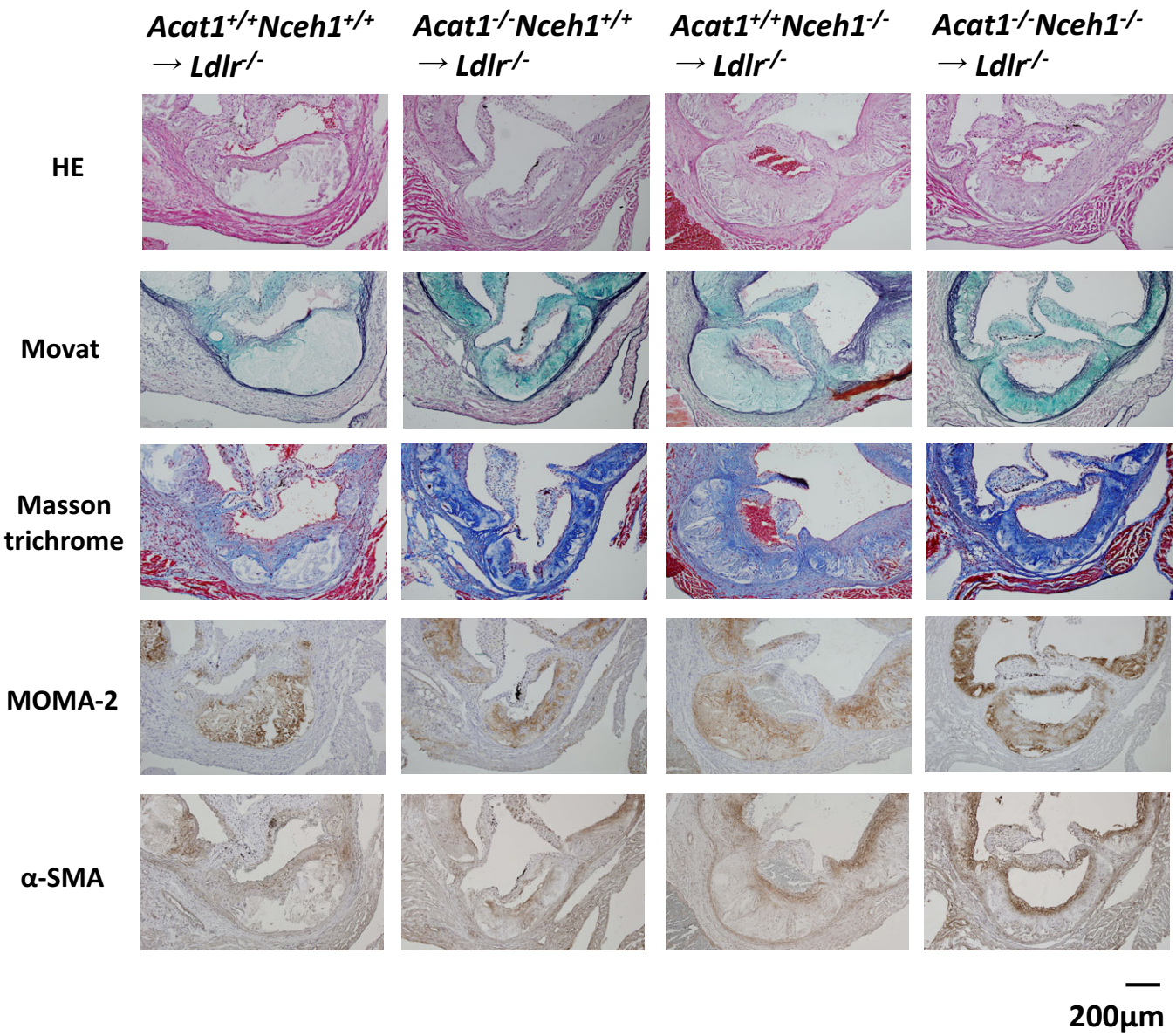

Fig. 2. Morphological comparison of atherosclerotic lesions in the recipients of WT, *Acat1*$^{-/-}$, *Nceh1*$^{-/-}$, *Acat1*$^{-/-}$;*Nceh1*$^{-/-}$ bone marrow.

Representative images of aortic root stained with HE, Movat's pentachrome, Masson trichrome, antibodies against macrophages (MOMA-2) or vascular smooth muscle cells (α-SMA). The Movat's pentachrome stains nuclei and elastic fibers black, collagen yellow, mucins blue to green, muscle red, and fibrin intense red.

tive area of the recipients of the *Acat1*$^{-/-}$;*Nceh1*$^{-/-}$ bone marrow was significantly smaller than that of the *Nceh1*$^{-/-}$ bone marrow by 58% ($p<0.001$). HE staining was performed to estimate the size of the necrotic core (**Figs. 2** and **3B**). The percentages of the necrotic core of the recipients of *Acat1*$^{-/-}$ or *Acat1*$^{-/-}$;*Nceh1*$^{-/-}$ bone marrow were significantly smaller than those of the WT or the *Nceh1*$^{-/-}$ bone marrow ($p<0.001$).

Movat's pentachrome staining was performed to estimate the area filled with mucins (**Figs. 2** and **3C**). The percentages of the area filled with mucins of the recipients of *Acat1*$^{-/-}$ and *Acat1*$^{-/-}$;*Nceh1*$^{-/-}$ bone marrow were 2.2-fold and 1.9-fold larger than that of the WT bone marrow, respectively. There was no difference in the percentage between the recipients of the *Nceh1*$^{-/-}$ bone marrow and those of the WT bone marrow.

Masson trichrome staining was performed to estimate the amounts of collagen (**Figs. 2** and **3D**). The percentages of collagen area of the recipients of the

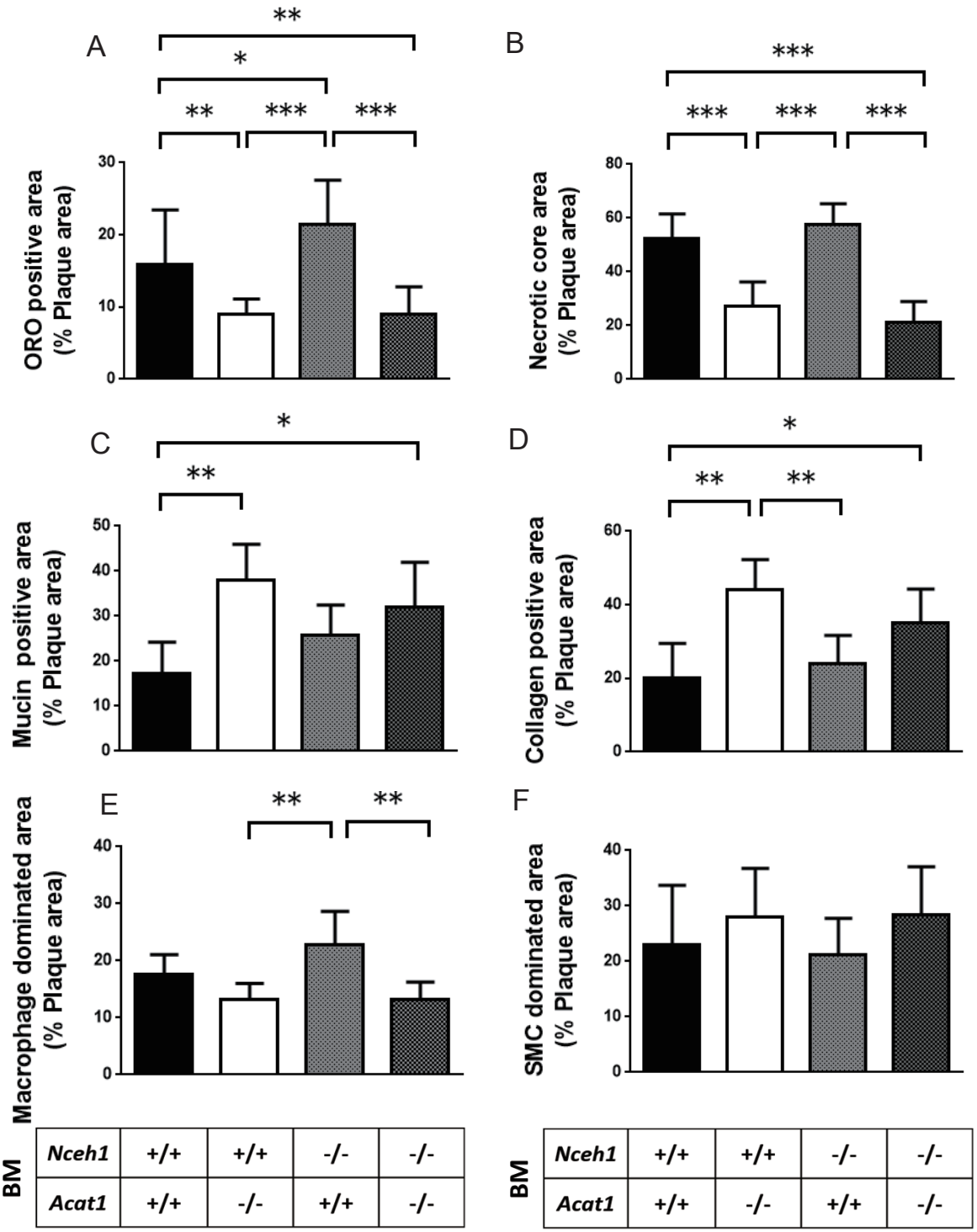

Fig. 3. Quantification of ORO-positive area (A), necrotic core area (B), mucin-positive area (C), collagen-positive area (D), macrophage-dominated area (E) and vascular smooth muscle cell-dominated area (F) in the atherosclerotic lesions in the recipients of WT, *Acat1*$^{-/-}$, *Nceh1*$^{-/-}$, *Acat1*$^{-/-}$;*Nceh1*$^{-/-}$ bone marrow.

(A) Quantification of ORO-positive area as a percentage of whole plaque area (n=13−18 animals per group). (B) Quantification of necrotic core from HE staining as a percentage of whole plaque area (n=6 animals per group). (C) Quantification of mucin-positive area from Movat's pentachrome (n=6 animals per group). (D) Quantification of collagen-positive area from Masson trichrome staining as a percentage of whole plaque area (n=5−6 animals per group). (E) Quantification of MOMA-2 positive area as a percentage of whole plaque area (n=5−6 animals per group). (F) Quantification of α-SMA positive area as a percentage of whole plaque area (n=5−6 animals per group). Values are expressed as means ± S.D. $^{*}p<0.05$, $^{**}p<0.01$, $^{***}p<0.001$.

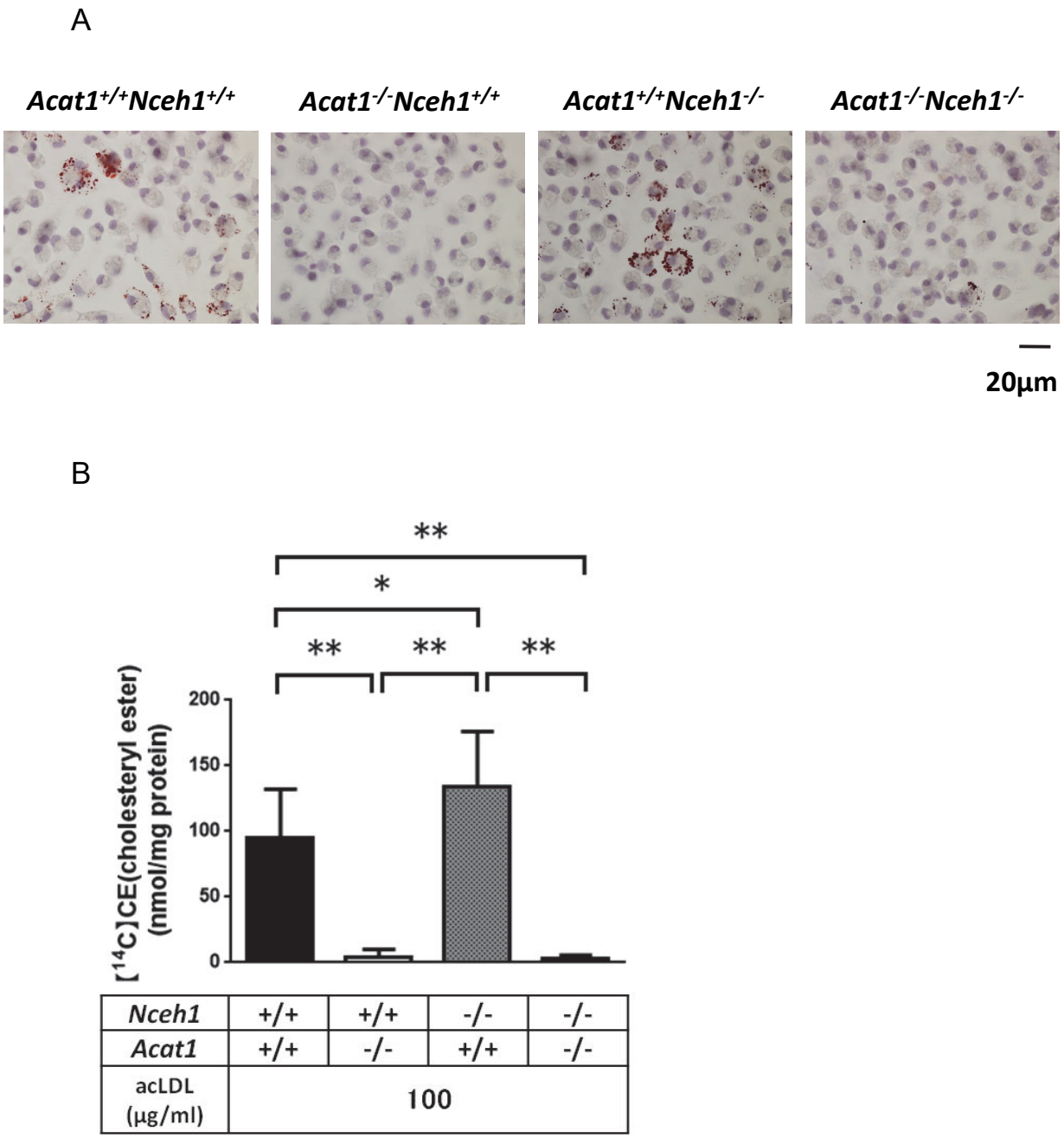

Fig. 4. Foam cell formation in WT, *Acat1*$^{-/-}$, *Nceh1*$^{-/-}$, *Acat1*$^{-/-}$;*Nceh1*$^{-/-}$ macrophages

Thioglycollate-elicited peritoneal macrophages were prepared from each mouse ($n=9-10$ animals per genotype). After macrophages were incubated with 100 μg/ml of acLDL for 24 h, ORO staining (A) and CE formation assay (B) were performed. Values are expressed as means ± S.D. $^{*}p<0.05$, $^{**}p<0.001$

Acat1$^{-/-}$ and *Acat1*$^{-/-}$;*Nceh1*$^{-/-}$ bone marrow were 2.2-fold and 1.7-fold larger than that of the WT bone marrow, respectively. There was no difference in the percentage of collagen-positive area between the recipients of *Nceh1*$^{-/-}$ bone marrow and those of the WT bone marrow.

Immunostaining for MOMA-2 was performed to estimate macrophage contents (**Figs. 2** and **3E**). The percentage of macrophage content in the recipients of the *Nceh1*$^{-/-}$ bone marrow tended to be larger than that of the WT bone marrow; however, the difference was not statistically significant.

Immunostaining for α-SMA was performed to estimate the distribution and amounts of vascular smooth

muscle cells (VSMCs) (**Figs. 2** and **3F**). α-SMA-positive cells were primarily distributed in the subendothelial areas and media. There were no differences in the amounts of the α-SMA-positive cells among the four types of mice.

Next, we compared the ORO staining (**Fig. 4A**), the amounts of CE formed from oleate (**Fig. 4B**) in peritoneal macrophages cultured in the presence of 100 μg/ml acLDL in the medium for 24 h among the four types of mice. Numerous ORO-positive lipid droplets were observed in WT and Nceh1-deficient macrophages, while they were barely detectable in *Acat1*$^{-/-}$ and *Acat1*$^{-/-}$*;Nceh1*$^{-/-}$ macrophages (**Fig. 4A**). The CE formation was drastically reduced to almost undetectable level in both *Acat1*$^{-/-}$ and *Acat1*$^{-/-}$*;Nceh1*$^{-/-}$ macrophages (**Fig. 4B**). The CE formation in *Nceh1*$^{-/-}$ macrophages was 1.4-fold higher than that in the WT macrophages ($p<0.05$).

Discussion

In the present study, we show that loss of both ACAT1 and NCEH1 in the bone marrow-derived cells reversed the size of the cross-sectional atherosclerotic lesion area which was aggravated by the loss of NCEH1 in the bone marrow-derived cells in *Ldlr*$^{-/-}$ after feeding with HCD. In parallel, the loss of both ACAT1 and NCEH1 decreased the ORO-positive area, macrophage content and necrotic area, which were worsened by the loss of NCEH1. These results provide *in vivo* proof of our premise that NCEH1 mediates the hydrolysis of CE, which is counteracted by the action of ACAT1, cholesterol esterification, in macrophages. The loss of ACAT1 may abrogate the pro-atherogenic effects of loss of NCEH1 by suppressing the supply of its substrate, FC. Since the differences in the ORO-positive area among the different genotypes of mice (**Fig. 3A**) were largely proportional to the differences in CE contents of the macrophages in culture (**Fig. 4A** and **4B**), the ORO-positive area may faithfully reflect the degree of CE accumulation in each macrophage in this model.

It is worth discussing the data which were apparently different from those reported by previous reports, including ours. In the present study, first, the cross-sectional lesion area of the recipients of the *Acat1*$^{-/-}$ bone marrow was not different from those of the WT bone marrow (**Fig. 1**). This was apparently inconsistent with the results of *en face* lesion size (**Supplemental Fig. 3**) and those reported by Fazio *et al.* in which the lesions of the recipients of the *Acat1*$^{-/-}$ bone marrow were larger than those of the WT bone marrow[22, 23]. Although we and Fazio *et al.* used the same diet (1.25% cholesterol), we fed the mice longer than Fazio *et al.* did (12 w vs 10 w). Potential reasons for the inconsistency may be the difference in the duration of the feeding with HCD and other unknown factors. However, the histological analyses showed that the mucin-positive and collagen-positive area were enlarged in the lesions of the recipients of the *Acat1*$^{-/-}$ bone marrow compared with those of the WT bone marrow (**Figs. 2** and **3CD**), indicating that increased production of mucin, complex mixtures of glycosaminoglycans and proteoglycans secreted from VSMCs[24], and increased fibrosis. Similar stimulation of fibrosis was reported in *apoE*-null mice treated with K-604, ACAT1 selective inhibitor[25].

It is also puzzling to note that the results of the recipients of the *Acat1*$^{-/-}$ bone marrow were inconsistent between the cross sectional and *en face* analyses (**Fig. 1** and **Supplemental Fig. 3**). Site-specific discrepancy has been reported in several studies examining the effects of drugs on the lesions. For example, pravastatin inhibited the lesions at brachiocephalic arteries and aortic roots, but not on the surface of the aorta[26]. Although the precise reasons are unknown, we speculate that the stage of the lesions which are dependent on age or the duration of feeding with HCD is a potential contributing factor. Our preliminary study showed that the lesions of the aortic roots of the recipients of *Acat1*$^{-/-}$ bone marrow were larger than those of the recipients of the WT bone marrow at 2 months of feeding, which are apparently similar to the results of the surface lesions at 3 months of feeding in the current study (**Supplemental Fig. 3**). It is well known that the lesions develop at aortic roots first and progress distally to thoracic, abdominal aorta, and iliac arteries[27]. Therefore, it is reasonable to speculate that the stage of the lesions of the aortic roots were more advanced than that of the aortic surface. Since the lesions of the recipients of the *Acat1*$^{-/-}$ or *Acat1*$^{-/-}$*;Nceh1*$^{-/-}$ bone marrow were much more fibrotic than the recipients of the WT or *Nceh1*$^{-/-}$ bone marrow, the expansion of the lesions of the recipients of the *Acat1*$^{-/-}$ or *Acat1*$^{-/-}$*;Nceh1*$^{-/-}$ bone marrow might be halted by fibrosis at a certain stage between 2 and 3 months of feeding, whereas the expansion of the lesions of the recipients of the WT or *Nceh1*$^{-/-}$ bone marrow might not be restricted by fibrosis. Although we did not examine the pathology of the lesion of the aortic surface, they might reflect the earlier stage than those at the aortic root, thus, sparing the restrictive effects of extensive fibrosis at later stages.

Theoretically, the cells positive for ORO staining should not be derived from bone marrow cells which lack ACAT1. Therefore, the ORO-positive cells observed in the recipients of the *Acat1*$^{-/-}$ bone marrow might be originated from the VSMCs of the recipients, because the VSMCs can be transformed to cells with macro-

phage-like property[28]. The loss of ACAT1 in macrophages of the donors might stimulate transformation of VSMCs of the recipients into macrophage-like cells, thereby, causing apparent enlargement of ORO-positive area. Staining for α-SMA showed that only the subendothelial areas contained VSMCs and the intensity of ORO staining was not different between the VSMC-dominant areas and the macrophage-dominant areas (**Figs. 1** and **2**). Therefore, it is more likely that lipoproteins deposited in extra-cellular matrix (ECM) are positive for ORO staining in the recipients of the *Acat1*$^{-/-}$ or *Acat1*$^{-/-}$*;Nceh1*$^{-/-}$ bone marrow. More studies are needed to determine the identity of the ORO-positive cells/or ECM in the recipients of the *Acat1*$^{-/-}$ bone marrow.

Conflicting results have been reported regarding the effects of the inhibition of ACAT1 on the atherosclerosis. In contrast to the mouse model of bone marrow transplantation mentioned above, models of systemic[12] and myeloid cell-specific deletion of ACAT1[29] and most of pharmacological studies using non-selective and selective ACAT1 inhibitors have shown the protection against atherosclerosis[30-35]. Although, currently, precise reasons are unknown, we would speculate that the type of non-macrophage cells whose ACAT1 is inhibited is a crucial determinant. According to Rong *et al.*[36], for example, the inhibition of ACAT1 is non-toxic in VSMCs and, thus, protects against atherosclerosis. Based on the premise, if the contribution of VSMCs to the atherosclerosis dominates over that of the bone marrow-derived cells, global knockout, and pharmacological inhibition of ACAT1 may be anti-atherogenic. According to Yang *et al.*[37], the inhibition of ACAT1 potentiates effector function and proliferation of pro-atherogenic CD8$^+$ T cells[38]. If this is the case, the pro-atherogenic effects of ACAT1 inactivation in the bone marrow-derive cells can be attributable to the phenotypes of this lymphoid lineage. Together, it is plausible that the role of ACAT1 inhibition in atherogenesis might be dependent on the cell types. Further studies are warranted to define the role ACAT1 in each type of cell in the development of atherosclerosis.

Moreover, the current results suggest that the roles of ACAT1 inhibition in atherogenesis are facet-specific. The loss of ACAT1 in the bone marrow-derived cells seems anti-atherogenic judged by the reduced number of foam cells (**Fig. 3A**) and increased deposition of collagen which is thought to stabilize plaques (**Fig. 3D**). Under such a condition as NCEH1-deficiency where foam cell formation is dominant, ACAT1 inhibition is likely to be anti-atherogenic. On the other hand, ACAT1 inhibition can be pro-atherogenic judged by the enlargement of mucin-positive area (**Fig. 3C**). Cell death can be both pro-atherogenic and anti-atherogenic depending on the contexts. If the surrounding cells have sufficient capacity to clear the dead cells, cell death will lead to involution of the plaque, thus, anti-atherogenic; if not, the presence of dead cells elicits inflammation, thereby, recruiting more inflammatory cells and transforming VSMCs to macrophage-like cells, thus, pro-atherogenic. Probably, all of these are the reasons why clinical trials have not been successful to inhibit the plaque volume in the coronary arteries[39-41].

Conclusion

Loss of ACAT1 in bone marrow-derived cells attenuates atherosclerosis, which is aggravated by loss of NCEH1. These results are in agreement with the *in vitro* functions of ACAT1 (formation of CE) and NCEH1 (hydrolysis of CE).

Acknowledgments

We thank Mika Hayashi and Nozomi Takatsuto for the excellent technical assistance.

Notice of Grant Support

This work was supported by Program for the Strategic Research Foundation at Private Universities 2011-2015 “Cooperative Basic and Clinical Research on Circadian Medicine” and “Non-communicable diseases (NCD)” from the Ministry of Education, Culture, Sports, Science and Technology of Japan, and unrestricted grants from Astellas Pharma, Daiichi Sankyo Co., Shionogi Co., Boehringer Ingelheim Japan, Mitsubishi Tanabe Pharma, Ono Pharma, Kowa Pharma, Takeda Pharma Co, Toyama Chemical Co., Teijin, Sumitomo Dainippon Pharma, Sanofi K.K., Novo Nordisk Pharma, MSD K.K., Pfizer Japan, Novartis Pharma and Eli Lilly Co.

Conflicts of Interests

There is nothing to disclose with regard to this topic.

Footnotes Added in the Proof

The present addresses of the following authors are as follows: K.S., Department of Dermatology and Cutaneous Surgery, Miami Itch Center, University of Miami Miller School of Medicine, Miami, FL, USA; H.Y., Department of Endocrinology and Metabolism, Mito Medical Center, Tsukuba University Hospital Mito Kyodo General Hospital, Ibaraki, Japan; M.S., Department of Internal Medicine (Endocrinology and

Metabolism), Faculty of Medicine, University of Tsukuba, Ibaraki, Japan.

References

1) Cochain C, Zernecke A. Macrophages in vascular inflammation and atherosclerosis. Pflugers Arch. 2017; 469: 485-499
2) Chang TY, Li BL, Chang CC, Urano Y. Acyl-coenzyme A: cholesterol acyltransferases. Am J Physiol Endocrinol Metab. 2009; 297: E1-9
3) Brown MS, Ho YK, Goldstein JL. The cholesteryl ester cycle in macrophage foam cells. Continual hydrolysis and re-esterification of cytoplasmic cholesteryl esters. J Biol Chem. 1980; 255: 9344-9352
4) Sekiya M, Osuga J, Igarashi M, Okazaki H, Ishibashi S. The role of neutral cholesterol ester hydrolysis in macrophage foam cells. J Atheroscler Thromb. 2011; 18: 359-364
5) Ouimet M, Marcel YL. Regulation of lipid droplet cholesterol efflux from macrophage foam cells. Arterioscler Thromb Vasc Biol. 2012; 32: 575-581
6) Okazaki H, Igarashi M, Nishi M, Sekiya M, Tajima M, Takase S, Takanashi M, Ohta K, Tamura Y, Okazaki S, Yahagi N, Ohashi K, Amemiya-Kudo M, Nakagawa Y, Nagai R, Kadowaki T, Osuga J, Ishibashi S. Identification of neutral cholesterol ester hydrolase, a key enzyme removing cholesterol from macrophages. J Biol Chem. 2008; 283: 33357-33364
7) Igarashi M, Osuga J, Isshiki M, Sekiya M, Okazaki H, Takase S, Takanashi M, Ohta K, Kumagai M, Nishi M, Fujita T, Nagai R, Kadowaki T, Ishibashi S. Targeting of neutral cholesterol ester hydrolase to the endoplasmic reticulum via its N-terminal sequence. J Lipid Res. 2010; 51: 274-285
8) Igarashi M, Osuga J, Uozaki H, Sekiya M, Nagashima S, Takahashi M, Takase S, Takanashi M, Li Y, Ohta K, Kumagai M, Nishi M, Hosokawa M, Fledelius C, Jacobsen P, Yagyu H, Fukayama M, Nagai R, Kadowaki T, Ohashi K, Ishibashi S. The critical role of neutral cholesterol ester hydrolase 1 in cholesterol removal from human macrophages. Circ Res. 2010; 107: 1387-1395
9) Sekiya M, Osuga J, Nagashima S, Ohshiro T, Igarashi M, Okazaki H, Takahashi M, Tazoe F, Wada T, Ohta K, Takanashi M, Kumagai M, Nishi M, Takase S, Yahagi N, Yagyu H, Ohashi K, Nagai R, Kadowaki T, Furukawa Y, Ishibashi S. Ablation of neutral cholesterol ester hydrolase 1 accelerates atherosclerosis. Cell Metab. 2009; 10: 219-228
10) Sakai K, Igarashi M, Yamamuro D, Ohshiro T, Nagashima S, Takahashi M, Enkhtuvshin B, Sekiya M, Okazaki H, Osuga J, Ishibashi S. Critical role of neutral cholesteryl ester hydrolase 1 in cholesteryl ester hydrolysis in murine macrophages. J Lipid Res. 2014; 55: 2033-2040
11) Osuga J, Ishibashi S, Oka T, Yagyu H, Tozawa R, Fujimoto A, Shionoiri F, Yahagi N, Kraemer FB, Tsutsumi O, Yamada N. Targeted disruption of hormone-sensitive lipase results in male sterility and adipocyte hypertrophy, but not in obesity. Proc Natl Acad Sci U S A. 2000; 97: 787-792
12) Yagyu H, Kitamine T, Osuga J, Tozawa R, Chen Z, Kaji Y, Oka T, Perrey S, Tamura Y, Ohashi K, Okazaki H, Yahagi N, Shionoiri F, Iizuka Y, Harada K, Shimano H, Yamashita H, Gotoda T, Yamada N, Ishibashi S. Absence of CAT-1 attenuates atherosclerosis but causes dry eye and cutaneous xanthomatosis in mice with congenital hyperlipidemia. J Biol Chem. 2000; 275: 21324-21330
13) Ishibashi S, Brown MS, Goldstein JL, Gerard RD, Hammer RE, Herz J. Hypercholesterolemia in low density lipoprotein receptor knockout mice and its reversal by adenovirus-mediated gene delivery. J Clin Invest. 1993; 92: 883-893
14) Usui S, Hara Y, Hosaki S, Okazaki M. A new on-line dual enzymatic method for simultaneous quantification of cholesterol and triglycerides in lipoproteins by HPLC. J Lipid Res. 2002; 43: 805-814
15) Paigen B, Morrow A, Holmes PA, Mitchell D, Williams RA. Quantitative assessment of atherosclerotic lesions in mice. Atherosclerosis. 1987; 68: 231-240
16) Movat HZ. Demonstration of all connective tissue elements in a single section; pentachrome stains. AMA Arch Pathol. 1955; 60: 289-295
17) Ishibashi S, Goldstein JL, Brown MS, Herz J, Burns DK. Massive xanthomatosis and atherosclerosis in cholesterol-fed low density lipoprotein receptor-negative mice. J Clin Invest. 1994; 93: 1885-1893
18) Usui F, Shirasuna K, Kimura H, Tatsumi K, Kawashima A, Karasawa T, Hida S, Sagara J, Taniguchi S, Takahashi M. Critical role of caspase-1 in vascular inflammation and development of atherosclerosis in western diet-fed apolipoprotein E-deficient mice. Biochem Biophys Res Commun. 2012; 425: 162-168
19) Havel RJ, Eder HA, Bragdon JH. The distribution and chemical composition of ultracentrifugally separated lipoproteins in human serum. J Clin Invest. 1955; 34: 1345-1353
20) Goldstein JL, Ho YK, Basu SK, Brown MS. Binding site on macrophages that mediates uptake and degradation of acetylated low density lipoprotein, producing massive cholesterol deposition. Proc Natl Acad Sci U S A. 1979; 76: 333-337
21) Ishibashi S, Inaba T, Shimano H, Harada K, Inoue I, Mokuno H, Mori N, Gotoda T, Takaku F, Yamada N. Monocyte colony-stimulating factor enhances uptake and degradation of acetylated low density lipoproteins and cholesterol esterification in human monocyte-derived macrophages. J Biol Chem. 1990; 265: 14109-14117
22) Fazio S, Major AS, Swift LL, Gleaves LA, Accad M, Linton MF, Farese RV, Jr. Increased atherosclerosis in LDL receptor-null mice lacking ACAT1 in macrophages. J Clin Invest. 2001; 107: 163-171
23) Su YR, Dove DE, Major AS, Hasty AH, Boone B, Linton MF, Fazio S. Reduced ABCA1-mediated cholesterol efflux and accelerated atherosclerosis in apolipoprotein E-deficient mice lacking macrophage-derived ACAT1. Circulation. 2005; 111: 2373-2381
24) Emoto N, Onose H, Yamada H, Minami S, Tsushima T, Wakabayashi I. Growth factors increase pericellular proteoglycans independently of their mitogenic effects on A10 rat vascular smooth muscle cells. Int J Biochem Cell Biol. 1998; 30: 47-54
25) Yoshinaka Y, Shibata H, Kobayashi H, Kuriyama H,

Shibuya K, Tanabe S, Watanabe T, Miyazaki A. A selective ACAT-1 inhibitor, K-604, stimulates collagen production in cultured smooth muscle cells and alters plaque phenotype in apolipoprotein E-knockout mice. Atherosclerosis. 2010; 213: 85-91
26) Kostogrys RB, Franczyk-Zarow M, Gasior-Glogowska M, Kus E, Jasztal A, Wrobel TP, Baranska M, Czyzynska-Cichon I, Drahun A, Manterys A, Chlopicki S. Anti-atherosclerotic effects of pravastatin in brachiocephalic artery in comparison with en face aorta and aortic roots in ApoE/LDLR$^{-/-}$ mice. Pharmacol Rep. 2017; 69: 112-118
27) Ma Y, Wang W, Zhang J, Lu Y, Wu W, Yan H, Wang Y. Hyperlipidemia and atherosclerotic lesion development in LDLR-deficient mice on a long-term high-fat diet. PLoS One. 2012; 7: e35835
28) Shankman LS, Gomez D, Cherepanova OA, Salmon M, Alencar GF, Haskins RM, Swiatlowska P, Newman AA, Greene ES, Straub AC, Isakson B, Randolph GJ, Owens GK. KLF4-dependent phenotypic modulation of smooth muscle cells has a key role in atherosclerotic plaque pathogenesis. Nat Med. 2015; 21: 628-637
29) Huang LH, Melton EM, Li H, Sohn P, Rogers MA, Mulligan-Kehoe MJ, Fiering SN, Hickey WF, Chang CC, Chang TY. Myeloid acyl-CoA: cholesterol acyltransferase 1 deficiency reduces lesion macrophage content and suppresses atherosclerosis progression. J Biol Chem. 2016; 291: 6232-6244
30) Bocan TM, Krause BR, Rosebury WS, Mueller SB, Lu X, Dagle C, Major T, Lathia C, Lee H. The ACAT inhibitor avasimibe reduces macrophages and matrix metalloproteinase expression in atherosclerotic lesions of hypercholesterolemic rabbits. Arterioscler Thromb Vasc Biol. 2000; 20: 70-79
31) Kusunoki J, Hansoty DK, Aragane K, Fallon JT, Badimon JJ, Fisher EA. Acyl-CoA: cholesterol acyltransferase inhibition reduces atherosclerosis in apolipoprotein E-deficient mice. Circulation. 2001; 103: 2604-2609
32) Delsing DJ, Offerman EH, van Duyvenvoorde W, van Der Boom H, de Wit EC, Gijbels MJ, van Der Laarse A, Jukema JW, Havekes LM, Princen HM. Acyl-CoA: cholesterol acyltransferase inhibitor avasimibe reduces atherosclerosis in addition to its cholesterol-lowering effect in apoE*3-leiden mice. Circulation. 2001; 103: 1778-1786
33) Namatame I, Tomoda H, Ishibashi S, Omura S. Antiatherogenic activity of fungal beauveriolides, inhibitors of lipid droplet accumulation in macrophages. Proc Natl Acad Sci U S A. 2004; 101: 737-742
34) Terasaka N, Miyazaki A, Kasanuki N, Ito K, Ubukata N, Koieyama T, Kitayama K, Tanimoto T, Maeda N, Inaba T. ACAT inhibitor pactimibe sulfate (CS-505) reduces and stabilizes atherosclerotic lesions by cholesterol-lowering and direct effects in apolipoprotein E-deficient mice. Atherosclerosis. 2007; 190: 239-247
35) Ikenoya M, Yoshinaka Y, Kobayashi H, Kawamine K, Shibuya K, Sato F, Sawanobori K, Watanabe T, Miyazaki A. A selective ACAT-1 inhibitor, K-604, suppresses fatty streak lesions in fat-fed hamsters without affecting plasma cholesterol levels. Atherosclerosis. 2007; 191: 290-297
36) Rong JX, Kusunoki J, Oelkers P, Sturley SL, Fisher EA. Acyl-coenzyme A (CoA): cholesterol acyltransferase inhibition in rat and human aortic smooth muscle cells is nontoxic and retards foam cell formation. Arterioscler Thromb Vasc Biol. 2005; 25: 122-127
37) Yang W, Bai Y, Xiong Y, Zhang J, Chen S, Zheng X, Meng X, Li L, Wang J, Xu C, Yan C, Wang L, Chang CC, Chang TY, Zhang T, Zhou P, Song BL, Liu W, Sun SC, Liu X, Li BL, Xu C. Potentiating the antitumour response of CD8$^+$ T cells by modulating cholesterol metabolism. Nature. 2016; 531: 651-655
38) Cochain C, Koch M, Chaudhari SM, Busch M, Pelisek J, Boon L, Zernecke A. CD8$^+$ T cells regulate monopoiesis and circulating Ly6C^{high} monocyte levels in atherosclerosis in mice. Circ Res. 2015; 117: 244-253
39) Tardif JC, Gregoire J, L'Allier PL, Anderson TJ, Bertrand O, Reeves F, Title LM, Alfonso F, Schampaert E, Hassan A, McLain R, Pressler ML, Ibrahim R, Lesperance J, Blue J, Heinonen T, Rodes-Cabau J; for the Avasimibe and Progression of Lesions on UltraSound (A-PLUS) Investigators. Effects of the acyl coenzyme A: cholesterol acyltransferase inhibitor avasimibe on human atherosclerotic lesions. Circulation. 2004; 110: 3372-3377
40) Nissen SE, Tuzcu EM, Brewer HB, Sipahi I, Nicholls SJ, Ganz P, Schoenhagen P, Waters DD, Pepine CJ, Crowe TD, Davidson MH, Deanfield JE, Wisniewski LM, Hanyok JJ, Kassalow LM; for the ACAT Intravascular Atherosclerosis Treatment Evaluation (ACTIVATE) Investigators. Effect of ACAT inhibition on the progression of coronary atherosclerosis. N Engl J Med. 2006; 354: 1253-1263
41) Meuwese MC, de Groot E, Duivenvoorden R, Trip MD, Ose L, Maritz FJ, Basart DC, Kastelein JJ, Habib R, Davidson MH, Zwinderman AH, Schwocho LR, Stein EA; for the CAPTIVATE Investigators. ACAT inhibition and progression of carotid atherosclerosis in patients with familial hypercholesterolemia: The captivate randomized trial. JAMA. 2009; 301: 1131-1139

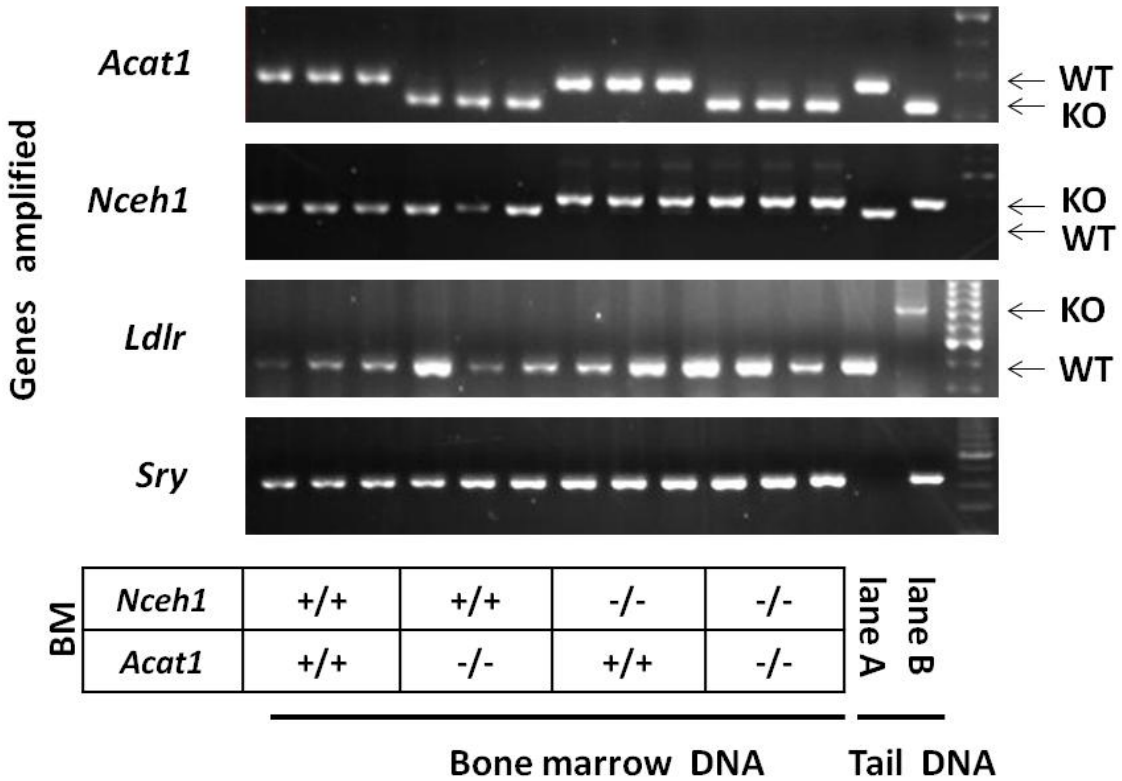

Supplemental Fig. 1. Successful reconstitution of the transplanted bone marrow

Bone marrow from mice with the indicated genotypes or tails (lane A and B) were used for isolation of genomic DNA. Tail DNA from a female WT mouse was used as a negative control for lane A of all the 4 gels. DNA isolated from the tails of *Acat1*$^{-/-}$, *Nceh1*$^{-/-}$, *Ldlr*$^{-/-}$ or male WT mouse was used as templates for PCR amplification of the mutant genes of *Acat1*, *Nceh1*, *Ldlr* or *Sry*, respectively. Respective PCR products were loaded to lane B of each gel.

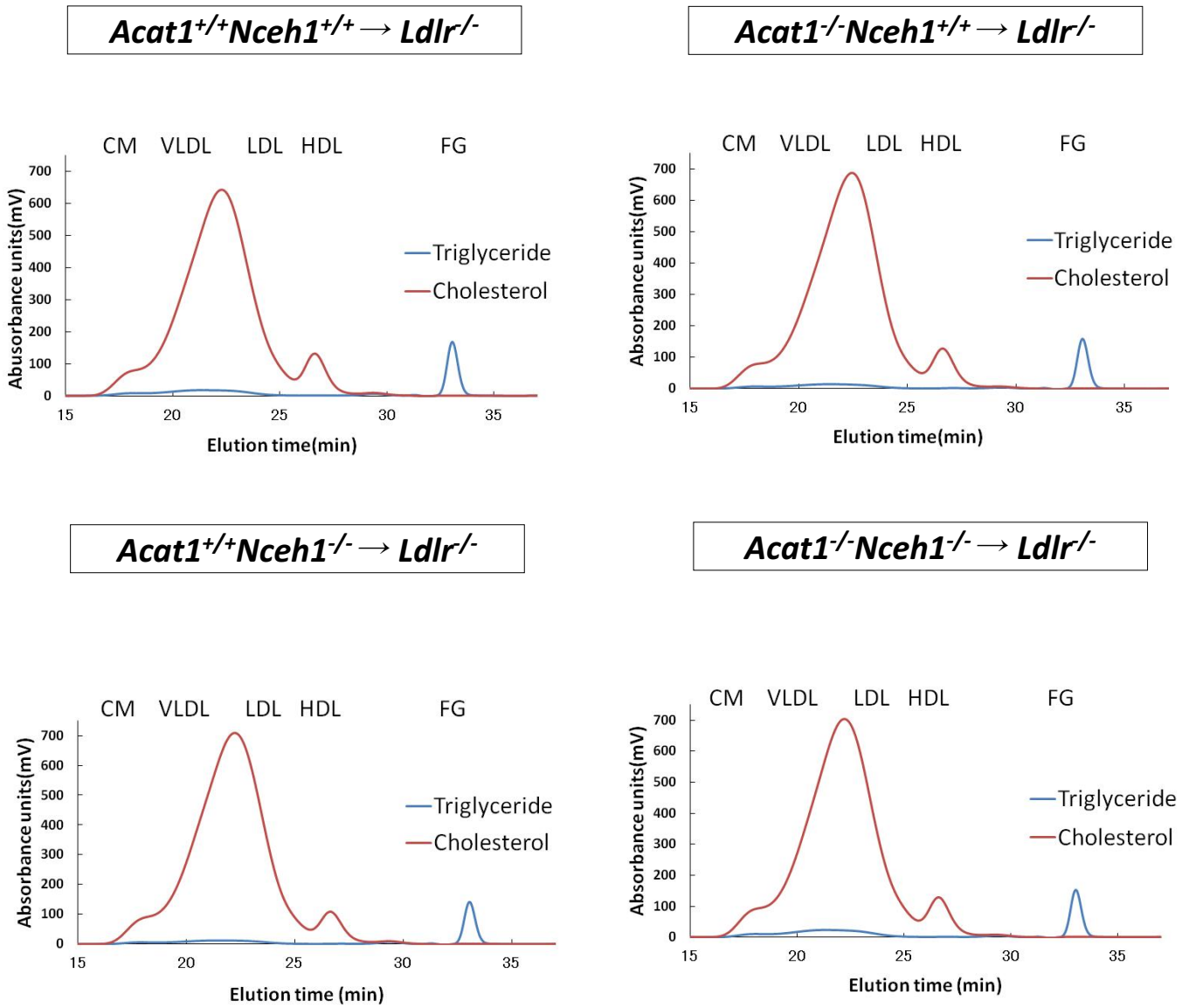

Supplemental Fig. 2. Lipoprotein profiles analyzed by HPLC

Mice (n=13−18) were fed a HCD diet for 12 weeks and plasma lipoprotein profiles were analyzed by HPLC. After a 16-h fast, blood samples were collected, pooled and subjected to HPLC.

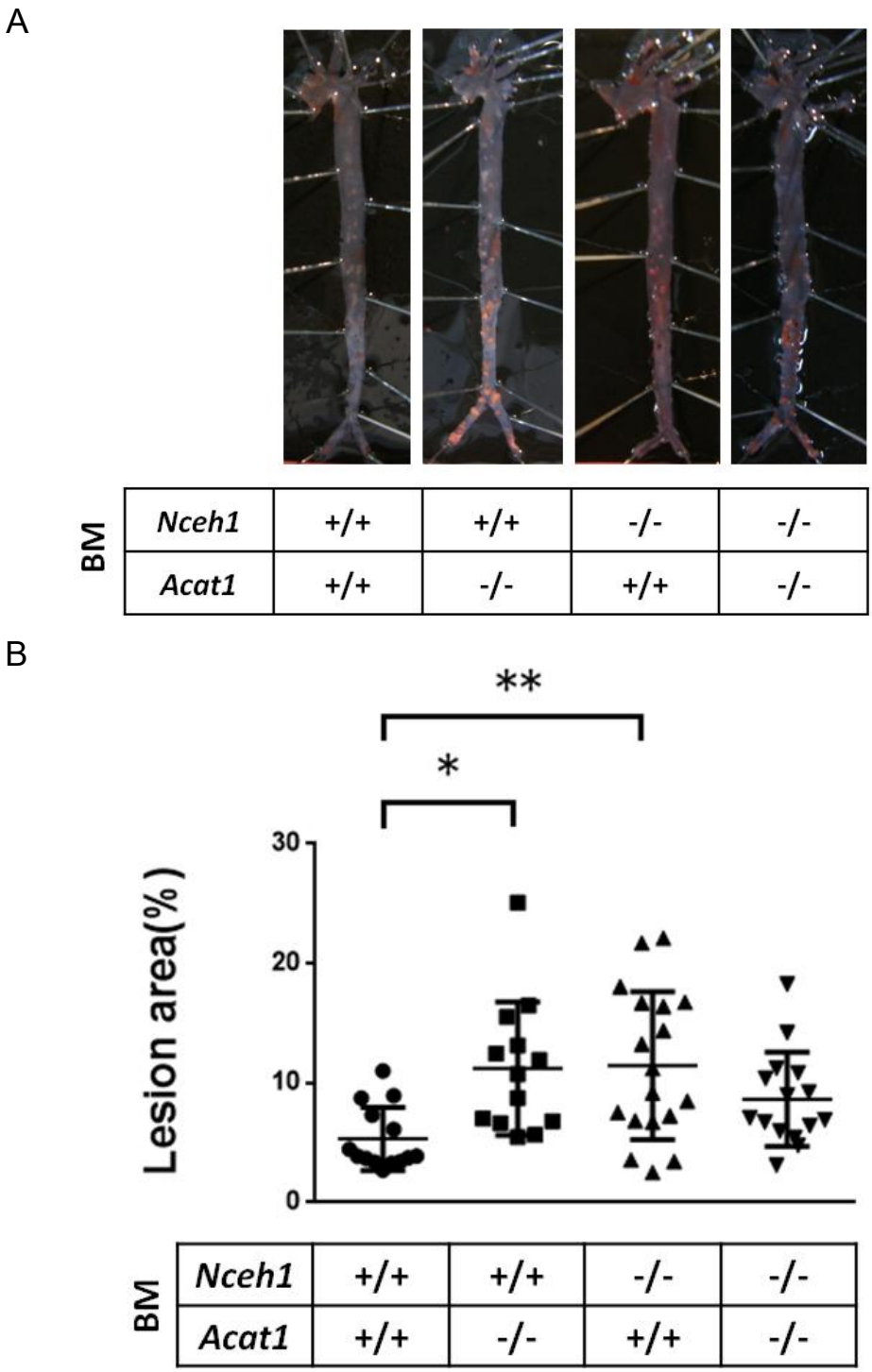

Supplemental Fig. 3. *En face* surface lesion areas of aorta in $Ldlr^{-/-}$ mice transplanted with WT, $Acat1^{-/-}$, $Nceh1^{-/-}$, $Acat1^{-/-}$;$Nceh1^{-/-}$ bone marrow.

The aorta of mice used for the experiment shown in Figs. 1-3 and Table 1 were stained with Sudan IV. (A) Representative macroscopic images. (B) Quantified lesion areas. The data was calculated as the percentage of surface lesion area of entire aorta. Values are expressed as means ± SD. $^{*}p<0.05$, $^{**}p<0.01$.